Chapter 1

Introduction

The finite element method (FEM) has become the most widely accepted general purpose technique for numerical simulations in engineering and applied mathematics. Principal applications arise in continuum mechanics, fluid flow, thermodynamics, and field theory. In these areas computational methods are essential and benefit strongly from the enormous advances in computer technology.

Splines play an important role in approximation and geometric modeling. They are used in data fitting, computer-aided design (CAD), automated manufacturing (CAM), and computer graphics. Extensive software is available, and algorithms are almost as efficient as for polynomials.

The early work of Schoenberg revealed that splines possess powerful approximation properties. Subsequently, many approximation schemes have been proposed. In particular, after de Boor's results about B-splines [2], spline techniques became popular for a broad range of applications. His algorithms are still the basic building blocks for almost any spline software. Another fundamental contribution is due to Bézier [1], who introduced modern piecewise polynomial modeling techniques to CAD/CAM. He recognized that the Bernstein basis yields a very intuitive geometric description of free form curves and surfaces, an important step being the knot insertion algorithms of Böhm and Riesenfeld et al [5]. This led to a revival of research on splines in the 1980s and considerably enriched the existing theory. As a consequence, B-splines became a standard not only for numerical approximation schemes, but also for free form design and geometry processing.

With geometric modeling and numerical simulation closely linked in engineering applications, the use of B-splines as finite element basis functions suggests itself. But, as is illustrated in Figure 1.1, at first sight this seems infeasible for two reasons:

(i) Essential boundary conditions cannot be modeled easily. For example, if a linear combination of B-splines, $p = \sum_k u_k b_k$, is required to vanish on the boundary ∂D of a domain *D,* then, in general, all coefficients u_k of B-splines with support intersecting ∂D must be 0. Hence, p equals 0 outside the light gray region in the figure, which results in very poor approximation order for solutions of Differential equations with Dirichlet boundary conditions.

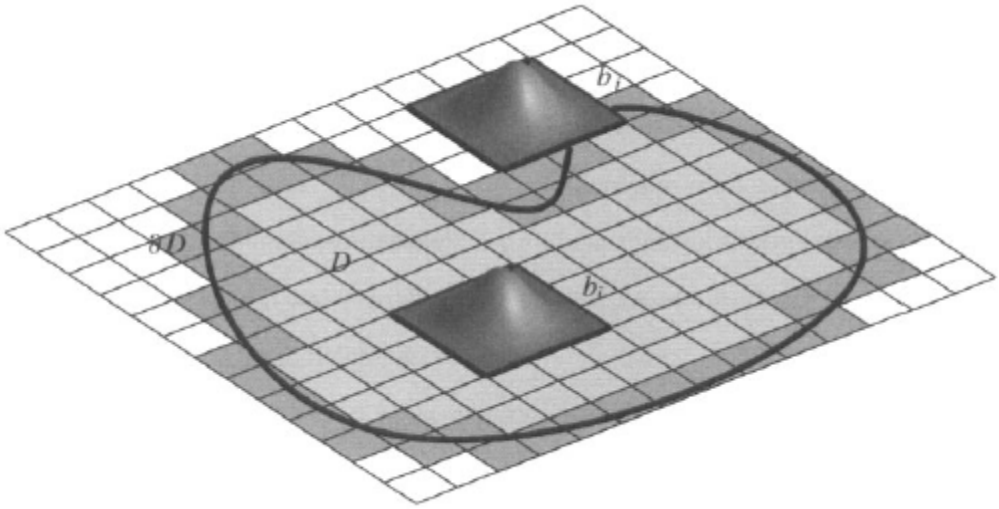

Figure1.1. Grid cells of biquadratic B-spline with support intersection a bounded domain.

(ii) The restricted B-spline basis is not uniformly stable. As shown in the figure, the basis may contain B-splines b_j with very small support in D consisting only of portions of the dark *gray* boundary grid cells. This leads to excessively large condition numbers of finite element systems and can cause extremely slow convergence of iterative methods.
The resulting methods combine the advantages of B-spline approximations on regular grids and standard mesh-based finite elements. They provide a natural link between geometric modeling and finite element methods.

The solution to the first of the above-mentioned problems is simple. Homogeneous essential boundary conditions can be modeled via weight functions, For example, solutions which vanish on ∂D are approximated with linear combinations of weighted B-splines:

$$wb_k, \qquad k \in K.$$

where K denotes indices of B-splines with some support in D and w is a smooth positive function on D with $w_{|\partial D} = 0$. The construction of such weight functions was extensively studied by Rvachev et al [6]. His R-function method (RFM) provides efficient algorithms for domains defined as Boolean combinations of elementary sets.

Resolving the stability problem, caused by the outer B-splines b_j, is slightly more subtle. A well-conditioned basis can be obtained by forming appropriate linear combinations

$$b_i + \sum_{j \in J(i)} e_{i,j} b_j, \qquad i \in I$$

The Inner indices $i \in I$ correspond to B-splines with at least one grid cell of their support contained in $\overline{D}$, and $j(i) \subset K \backslash I$ are small sets of neighboring outer indices j. These extended B-splines inherit all basic features of the standard B-splines b_i. In particular, their linear span maintains full approximation order

Combining the above ideas gives rise to the definition of weighted extended B-splines (web-splines). These basis functions possess the usual properties of standard finite elements. In addition, there are a number of algorithmic advantages of B-spline bases which lead to very efficient simulation techniques.

- No mesh generation is required.
- The uniform grid is ideally suited for parallelization and multigrid techniques.
- Accurate approximations are possible with relatively low-dimensional subspaces.
- Smoothness and approximation order can be chosen arbitrarily.
- Hierarchical bases permit adaptive refinement.

Given the difficulty of constructing finite element meshes, the first property is probably the most important one. Utilizing a regular grid not only eliminates a difficult preprocessing step, but also permits very efficient implementations of algorithms. Moreover, the use of B-splines reduces the dimension of finite element systems, in particular when high accuracy is required. Regardless of the degree, there is only one parameter for each grid cell.

Dependencies on parameters are not always indicated if they are clear from the context. For example, we write

$$b_k = b_{k,h}^n$$

for the m-variate tensor product B-spline of coordinate degree n, grid width h, and support $(k_1, \dots, k_m)h + [0, n+1]^m h$.

In estimates, the dependence of constants on parameters p_v is indicated in the form const $(p_1, p_2, \dots)$. If the dependence is clear from the context, or not particularly relevant, we use the symbols $\preccurlyeq, \succcurlyeq$ and $\asymp$. For example,

$$dist(x, \partial D) \underline{\succeq} h$$

Characterizes all points x with distance $\geq$ const h from the boundary of D.

A spline approximation $u_h$with grid width h of a function u is usually written in the form

$$u \approx u_h = \sum_k u_k b_k$$

And $U = \{u_k\}_{k \in K}$ is the vector of coefficients.

The terms vector and matrix are used in a broader sense. Their subscripts need not be integers. For example, for the Ritz-Galerkin matrices

$$G = \{g_{k,i}\}_{k,i \in I}$$

the indices are often integer vectors from a subset I of $\mathbb{Z}^m$. With this more general interpretation it is convenient not to distinguish between row and column vectors: i.e., a scalar product is written as UV without transposing one of the vectors.

We say that a function is smooth if it possesses the regularity required by the current context.. Using this convention, we do not have to keep track of the minimal number of required derivatives, which sometimes distracts from the essential arguments.

Slightly more restrictive than standard terminology, the term domain is used for a bounded open set $D \subset \mathbb{Z}^m$ with Lipschitz boundary.

Partial derivatives are denoted by

$$\partial_v u(x) = \frac{\partial}{\partial x_v} \mathrm{u(x)}.$$

For example,

$$grad\ u = (\partial_1 u, \dots, \partial_m u)$$

is the gradient of an m-variate function u,and $\Delta = \sum_{v=1}^{m} \partial_v^2$ is the Laplace operator.

The 2-norm for vectors and matrices is denoted by $\|\cdot\|$. Finally, $\|u\|_\ell$is the norm of a function u in the Sobolev space $H^\ell(D)$, corresponding to the scalar product $\langle\cdot,\cdot\rangle_\ell$ (cf. section 2.3).

Chapter 2
Basic Finite Element Concepts

2.1 A Model Problem

To explain the basic finite element idea, we consider Poisson's equation with homogeneous boundary conditions,

$$-\Delta u = f \text{ in } D, \quad u = 0 \text{ on } \partial D, \tag{2.1}$$

for a domain $D \subset \mathbb{R}^m$ as a model problem. This boundary value problem describes

a number of physical phenomema. A simple two-dimensional example is shown in Figure 2.1. An elastic membrane is fixed at its boundary ∂D and subjected to a vertical force with density$f$. If the resulting displacement $u(x_1, x_2)$ is small, it can be accurately modeled by Poisson's equation.

Multiplying the differential equation $-\Delta u = f$ by a smooth function v, which vanishes on the boundary, and integrating by parts, it follows that

$$\int_D \text{grad } u \text{ grad } v = \int_D fv, \qquad v_{|\partial D} = 0 \tag{2.2}$$

This weak form of Poisson's problem suggests a natural discretization. We approximate the solution u by a linear combination

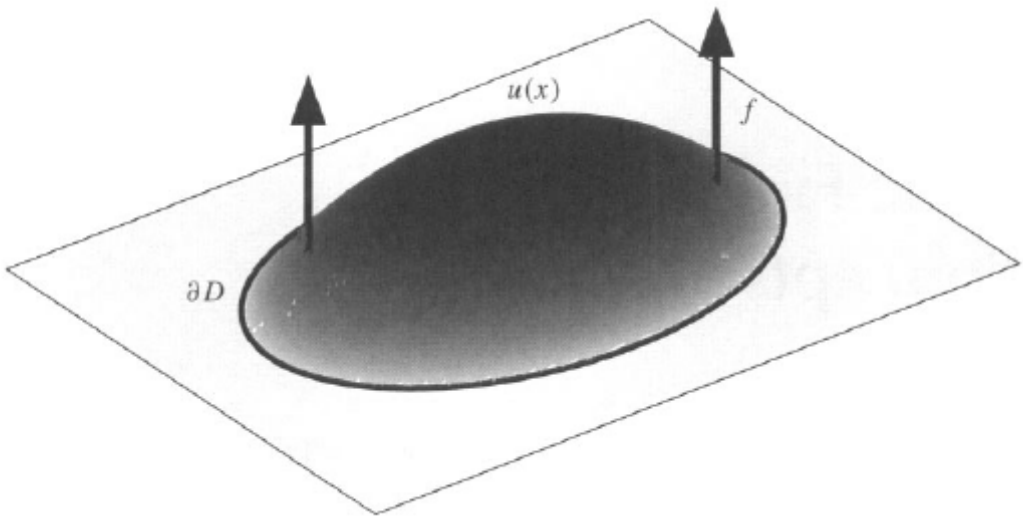

Figure 2.1. *Displacement (magnified) of an elastic membrane.*

$$u_h = \sum_{\mathrm{i}} \mathrm{u_i B_i}$$

of basis functions B_i which satisfy the boundary condition $B_{i|\partial D} = 0$. Usually, the "finite elements" B_i are piecewise polynomials with small support on a mesh of the domain D, and h denotes the maximum diameter of the mesh cells. Replacing u by u_h in (2.2) and choosing $v = B_k$, we obtain a linear system

$$\int_D grad\ (\sum_i u_i B_i)\ grad\ B_k = \int_D f B_k$$

for the coefficients $U = \{u_i\}$. We summarize this basic finite element scheme, which was first proposed by Ritz and Galerkin at the beginning of the 20th century, as follows.

The coefficients of a standard finite element approximation

$$u_h = \sum_i u_i B_i\ , \quad B_{i|\partial D} = 0$$

for the boundary value problem

$$-\Delta u = f\ , \quad u_{|\partial D} = 0$$

are determined from the linear system $GU = F$ with

$$\mathrm{g_{k.i}} = \int_D \mathrm{grad}\ B_i\ \ \mathrm{grad}\ B_k\ , \quad f_k = \int_D f\ B_k$$

The Ritz-Galerkin method can also be derived via a variational approach. To this end we note that a smooth solution u of Poisson's problem minimizes the energy functional

$$Q(u) = \tfrac{1}{2} \int_D \mathrm{grad}\ u\ \mathrm{grad}\ u - \int_D \mathrm{f\,u} \qquad (2.3)$$

over all smooth functions which vanish on ∂D. The characterization of a minimum,

$$Q(u) \le Q(u + tv) = Q(\mathrm{u}) + \ t\left[\int_D \mathrm{grad}\ u\ \mathrm{grad}\ v - fv\right] + \frac{t^2}{2}\int_D \mathrm{grad}\ v\ \mathrm{grad}v$$

Where $t \in \mathbb{R}$ is arbitrary, again leads to (2.2). Since the right-hand side is a parabola in t, the expression in square brackets must vanish for all admissible v.

We can define the finite element approximation by minimizing Q over the linear span

$$\mathbb{B}_h = \text{span}_i B_i$$

of the basis functions B_i. Expanding $Q(\sum_i u_i B_i)$ yields the quadratic form

$$Q(u_h) = \frac{1}{2} UGU - FU ,$$

Which is minimal if $GU = F$.

2.2 Mesh-Based Elements

We give in this section a brief overview of some typical classical finite elements.

Most commonly used finite elements are defined on a mesh, i.e., a partition of the domain D into triangles, quadrilaterals, tetrahedra, hexahedra, or other polygonal cells. Triangles and tetrahedra are preferred for most applications since they can be adapted more easily to complicated boundaries. In particular, generating hexahedral meshes in three dimensions is rather difficult. Often one has to resort to mixed partitions in order to overcome the geometric difficulties.

Figure 2.2 shows a triangulation of a two-dimensional domain with the hat-function. the basic piecewise linear finite element. A hat-function B_i equals 1 at an interior vertex x_i and vanishes on all triangles τ not containing x_i. Hence, the graph of B_i, is a pyramid

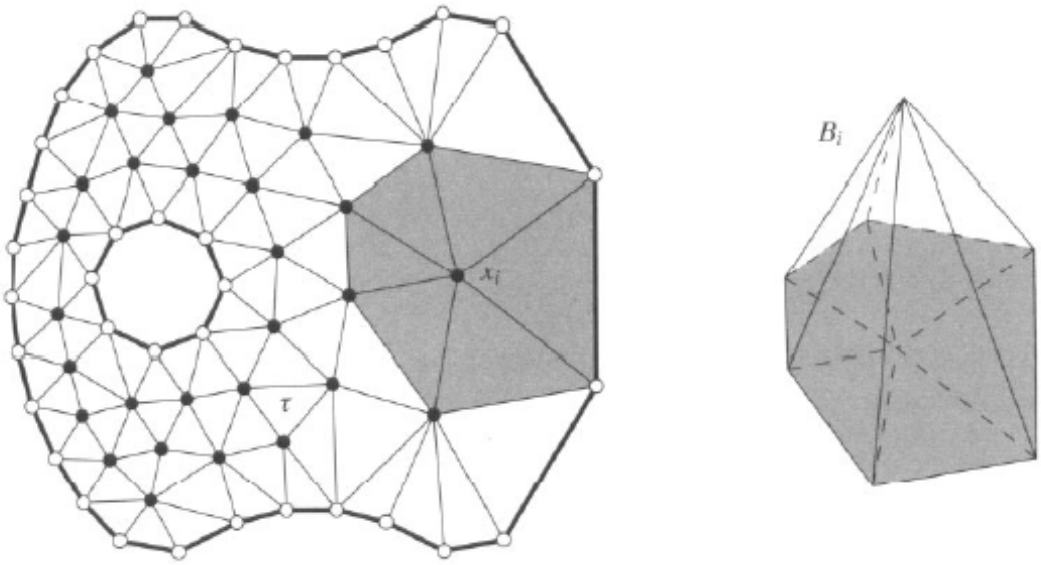

Figure 2.2. *Hat-function on a triangulation.*

with star-shaped support. For this very simple basis function, the coefficients u_i of an approximation

$$u_h = \sum_{\mathrm{i}} \mathrm{u_i B_i}$$

coincide with the values $u_h(x_i)$.

The Ritz-Galerkin approximation of Poisson's problem is easily computed. The linear system $GU = F$ is assembled by adding the contributions from each triangle τ of the triangulation, i.e.,

$$\mathrm{g}_{k,i} = \sum_{\tau} \int_{\tau} \mathrm{grad\ B_i\ grad B_k} \qquad f_k = \sum_{\tau} \int_{\tau} f\ \mathrm{B_k}$$

The gradients in the first integral are constant and can be determined by transforming the hat-functions to a standard reference triangle. For the entries of the right-hand side F numerical integration is used. Because of the small support of the hat-functions, the matrix G is sparse, and the Ritz-Galerkin system can be solved efficiently with iterative methods.

While simple to implement, piecewise linear finite element methods are not very accurate. In general, the error is at best of order $O(h^2)$. Where h is the maximum diameter of the triangles, Moreover, if standard triangulation algorithms

are used, homogeneous Dirichiet boundary conditions are fulfilled exactly essentially only for convex domains, Strictly speaking, B_i is not an admissible basis function if an edge of its support lies outside the domain D.

Better approximations can be obtained with polynomials of higher degree. Figure 2.3 gives a few examples of commonly used constructions. It is customary to describe these finite elements by the parameters which determine the polynomials on each triangle. Dots indicate values, circles gradients and second-order derivatives, and small marks on edges normal derivatives. For example, the data for the Argyris element consist of derivatives

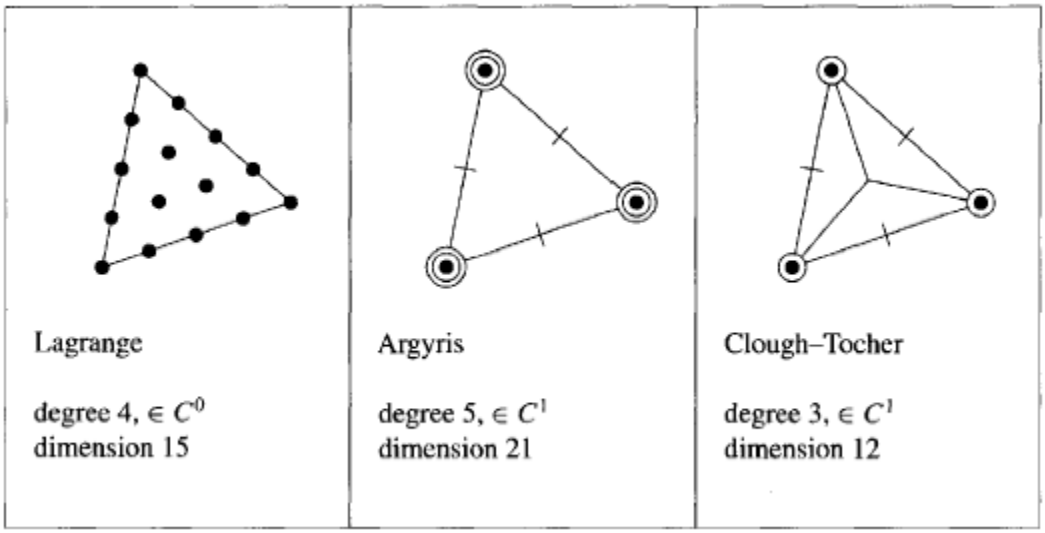

Figure 2.3. *Examples of bi variate finite elements.*

up to second order at each vertex and normal derivatives on the midpoints of each edge. The total number of parameters per triangle is $3(1 + 2 + 3) + 3 = 21$, which matches the dimension of quintic bivariate polynomials.

For each of the finite elements in Figure 2.3, the data shared *by adjacent* triangles are chosen to yield at least continuity across edges. This is necessary to permit the computation of gradients. For example, the approximations constructed with the quartic Lagrange element on the left are univariate quartic polynomials along each edge, which are uniquely determined by the live interpolated values. Hence, polynomials on adjacent triangles match, so that the bases functions are continuous ($B_i \in C^0$). Continuity of the gradient is more difficult to achieve. Either one has to resort to high polynomial degree or auxiliary subdivision, as is illustrated by the two examples on the right of the figure. For the Argyris triangle as well as for the Clough-Tocher element, the data associated with an edge

determine not only the polynomial but also its normal derivative along the edge uniquely. The corresponding basis functions have continuous first-order partial derivatives; i.e., they belong to C^1.

As for hat-functions, the data for finite element basis functions B_i, have exactly one nonzero entry. However, in general there are different types, depending on whether B_i is associated with an interpolated value or a derivative. For example, the Clough-Tocher finite element subspace is spanned by three basis functions B_i^α for each vertex x_i and one basis function B_k for each edge e_k. The functions B_i^α have support on the macro triangles sharing the vertex x_i. For $\alpha = (0,0)$ they equal 1 at x_i, and grad $B_j^\alpha(x_i) = (0,0)$; for α equal to $(1,0)\ or\ (0,1)$ they vanish at x_i with grad $B_i(x_i) = \alpha$. The function B_k has support on the macro triangles sharing the edge e_k and its normal derivative equals 1 at the midpoint of this edge.

Definition 2.1 (Properties of Finite Elements)
The bases functions B_i of standard mesh-based finite element subspaces are piecewise polynomials of degree $\leq n$ with support on few neighboring mesh cells. They are at least continuous and compatible with homogeneous boundary conditions.

2.3 Sobolev Spaces

For analyzing partial differential equations as well as numerical schemes, the choice of the appropriate function spaces is important. The classical theory of elliptic boundary value problems uses functions with Holder-continuous derivatives, requiring in particular that all terms appearing in the differential equations are continuous up to the boundary. However, this approach is limited to smooth problems and not well suited for finite element approximations. The natural framework for variational techniques becomes apparent when considering Poisson's problem

$$-\Delta u = f \quad in\ D, \qquad u = 0\ on\ \partial D$$

on the unit square $D = (0,1)^2$. For this special domain the solution is readily obtained by expanding the right-hand side into a Fourier series:

$$f = \sum_{k_1=1}^{\infty} \sum_{k_2=1}^{\infty} f_k \varphi_k, \qquad \varphi_k(x) = \sin(\pi k_1 x_1) \sin(\pi k_2 x_2)$$

Since the sine φ_k functions are eigenfunctions of the Laplace operator, i.e.,

$$-\Delta\varphi_k = \pi^2(k_1^2 + k_2^2)\varphi_k,$$

a comparison of coefficients yields

$$u_h = \frac{1}{\pi^2(k_1^2+k_2^2)} f_k \tag{2.4}$$

for the sine coefficients of $u = \sum_{k_1}\sum_{k_2} u_k\varphi_k$. This formal procedure is justified if f is square integrable:

$$f \in L_2(D) \Leftrightarrow \| f \|_0^2 = \int_D |f|^2 = \frac{1}{4}\sum_{k_1}\sum_{k_2} |f_k|^2 < \infty$$

By the standard theory of orthogonal expansions, the series for *f* and *u* converge in the scalar product norm $\| \cdot \|_0$. The coefficients of *u* decay more rapidly. From (2.4) we see that the sine coefficients of any second-order partial derivative $\partial_u\partial_\mu u$ are majorized by $\{f_k\}$:

$$(\pi k_v)(\pi k_\mu)|u_k| \le |f_k|.$$

Consequently,

$$f \in L_2(D) \Longrightarrow \partial_v\partial_\mu u \in L_2(D)$$

for all $v, \mu \in \{1,2\}$.

The space L_2 also arises in connection with the Poisson energy functional

$$Q(u) = \frac{1}{2}\int_D (|\partial_1 u|^2 + |\partial_2 u|^2) - \int_D \mathrm{f\,u}$$
$$= \frac{\pi^2}{8}\sum_{k_1}\sum_{k_2}(k_1^2 + k_2^2)|u_k|^2 - \frac{1}{4}\sum_{k_1}\sum_{k_2} f_k u_k\,,$$

which is well defined for functions with square integrable first-order partial derivatives:
$\partial_v u \in L_2(D)$. These considerations motivate the following definition.

Definition 2.2 (Sobolev Spaces)
The Sobolev space $H^\ell(D)$ consists of all functions u for which the partial derivatives of order $\leq \ell$

$$\partial^\alpha u = \partial_1^{\alpha_1} \dots \partial_m^{\alpha_m} u \ , \qquad |\alpha| = \alpha_1 + \cdots + \alpha_m \leq \ell,$$

are square integrable. It is a Hilbert space with the scalar product

$$\langle u, v \rangle_\ell = \sum_{|\alpha| \leq \ell} \int_D \partial^\alpha \mathrm{u}\, \partial^\alpha \mathrm{u}$$

In addition to the induced norm $\|u\|_\ell = \sqrt{\langle u, u \rangle_\ell}$ the standard semi-norm on H^ℓ is defined as

$$|u|_\alpha = \left(\sum_{|\alpha| = \ell} \int_D |\, \partial^\alpha \mathrm{u}|^2 \right)^{1/2}$$

i.e., it involves only derivatives of the highest order.

We have yet to define precisely what is meant by a square integrable derivative. This is done via integration by parts. We say that an integrable function $\partial^\alpha u$ is a weak derivative of u on a domain D if

$$\int_D (\partial^\alpha \mathrm{u}\,)\, \varphi = (-1)^{|\alpha|} \int_D u(\partial^\alpha \varphi\,)$$

for all smooth functions φ with compact support in D. This formula is obviously valid for smooth functions u. Hence, it is a proper extension of the standard definition of derivatives via difference quotients.

Sobolev spaces can also be defined as the closure of smooth functions with respect to the norm $\|.\|_\ell$. This confirms that H^ℓ is a Hilbert space. Moreover, many identities (such as integration by parts) can be conveniently derived by a limit process.

While the spaces H^ℓ are adequate for basic finite element analysis, it should

be mentioned that Sobolev spaces are defined more generally for p-integrable functions. The interplay between integrability, differentiability, and dimension gives rise to a very beautiful theory, which has become indispensable for studying partial differential equations.

For working with Sobolev spaces the regularity of the domain D is important. The commonly used hypothesis is that the boundary is Lipschftz-continuous, which we assume in what follows. This minimal requirement is satisfied by almost all applications of practical relevance. The domains of interest are usually more regular. They have piecewise smooth boundaries, and cusp-like singularities do not occur.

For approximating elliptic problems it is convenient to use Sobolev spaces which incorporate the boundary conditions. After reduction to homogeneous form they can be imposed as linear constraints.

Definition 2.3 (Sobolev Spaces with Boundary Conditions)
The subspace $H_0^\ell(D) \subset H^\ell$ consists of all functions which vanish on ∂D. More precisely. $H_0^\ell(D)$ is the closure of all smooth functions with compact support in D with respect to the norm $\|\cdot\|_\ell$.

There is a subtle point about boundary conditions for functions in Sobolev spaces. Since integrable functions can be modified on sets of measure zero (such as ∂D), offhand, boundary values are not well defined. However, we can use a limit process, as in the above definition. In this way, the restriction operator

$$u \to u_{|\partial D}$$

which is well defined for smooth functions, is generalized by continuous extension to $H^\ell(D)$.

2.4 Abstract Variational Problems

The finite element method can be formulated in a very general framework. Generalizing the model problem (2.1), we consider an abstract boundary value problem

$$\mathcal{L}u = f \text{ in } D,\ Bu = 0 \text{ on } \partial D,$$

with a differential operator $\mathcal{L}$ and an operator B describing the boundary conditions. Moreover, analogously to (2.2), we assume that this problem admits a variational formulation

$$a(u,v) = \lambda(v), \quad v \in H \tag{2.5}$$

where a is a bilinear form and λ is a linear functional on a Hilbert space H then, for a finite element subspace $\mathbb{B}_h \subset H$, the Ritz-Galerkin approximation u_h is defined by

$$a(u_h, v_h) = \lambda(v_h)\,, \; v_h \in \mathbb{B}_h, \tag{2.6}$$

The coefficients $u_i \;\; of \; u_h$ with respect to a basis B_i of $\mathbb{B}_h$ are determined via the linear system obtained by using $v_h = B_k$ as test functions.

Definition 2.4 (Ritz-Galerkin Approximation)
The Ritz-Galerkin approximation $u_h = \sum_i u_i B_i \in \mathbb{B}_h \subset H$, of the variational problem

$$a(u,v) = \lambda(v), \quad v \in H$$

is determined by the linear system

$$\sum_i a(B_i, B_k) u_i = \lambda(B_k),$$

which we abbreviate as $GU = F$.

For the model problem (2.1), $\mathcal{L}$ is the negative Laplace operator $-\Delta$, $\mathcal{B}u = u$, and

$$a(u,v) = \int_D \text{grad}\, u \,\text{grad}\, v\,, \quad \lambda(v) = \int_D fv\,.$$

The Hubert space H is the Sobolev space $H_0^1(D)$ of functions with square integrable first derivatives and zero boundary data, defined in 2.3. A simple finite element subspace $\mathbb{B}_h$ consists of piecewise linear functions on a triangulation of D, as described in section 2.2.

To analyze the abstract variational formulation of finite element approximations, the following property of the bilinear form a is crucial.

Definition 2.5 (Ellipticity)
A bilinear form a on a Hilbert space H is elliptic if it is bounded and equivalent to the norm on H. i.e., if for all $u, v \in H$

$$|a(u,v)| \leq c_b \|u\| \|v\|, \quad c_e \|u\|^2 \leq a(u,u)$$

with positive constants c_b and c_e.

For the Poisson bilinear form, the Cauchy-Schwarz inequality implies

$$\left| \int_D \text{grad } u \text{ grad } v \right| \leq \left(\int_D \|\text{grad} u\|^2 \right)^{1/2} \left(\int_D \|\text{grad} v\|^2 \right)^{1/2} \leq \|u\|_1 \|\text{v}\|_1 \ ,$$

where

$$\|w\|_1 = \left(\int_D |w|^2 \|\text{grad } w\|^2 \right)^{1/2}$$

is the norm on $H = H_0^1(D) \subset H^1(D)$. Hence, the constant c_b, in the upper bound equals 1 in this case. The lower bound is a consequence of the Poincaré-Friednchs inequality:

$$\int_D |u|^2 \leq const \int_D \|\text{grad } u\|^2 , \quad u \in H_0^1(D)$$

Adding $\int_D \|grad\ u\|^2 = a(u,u)$ to both sides, we see that $c_e = (cons(D) + 1)^{-1}$.

We now formulate the main existence result for elliptic variational problems [4].

Theorem 2.6 (Lax-Milgram)
If a is an elliptic bilinear form and λ is a bounded linear functional on a Hilbert space H, then the variational problem

$$a(u,v) = \lambda(v), \quad v \in H$$

has a unique solution $u\epsilon V$ for any closed subspace V of H. Moreover, if a is symmetric, the solution u can be characterized as the minimum of the quadratic form

$$Q(u) = \frac{1}{2}\, a(u\,, u) - \lambda(u)$$

On V.

For finite element approximations, the subspace $V = \mathbb{B}_h$, has finite dimension, and the variational problem is equivalent to the Ritz-Galerkin system $GU = F$, defined in *2.4* In this case, the duplicity of a implies that the matrix G is positive definite:

$$UGU = \sum_{i,k} u_k a(B_i, B_k) u_i = a(u_h, u_h) \geq c_e \|u_h\|^2 > 0$$

For $u_h \neq 0$. Hence, G is invertible and the Ritz-Galerkin system uniquely solvable, this simple observation already settles the part of the Lax- Milgram theorem relevant for numerical schemes.

2.5 Approximation Error

The error of finite element approximations u_h, can be related in a natural way to the error of the best approximation from the subspaces $\mathbb{B}_h$. This allows a priori estimates without any detailed knowledge about the differential equation or the Ritz—Galerkin solution. The crucial identity is the orthogonality relation

$$a(u - u_h, \omega_h) = 0, \quad \omega_h \in \mathbb{B}_\mathrm{h} \tag{2.7}$$

which follows by subtracting the Ritz-Galerkin equations (2.6) from the characterization (2.5) of weak solutions, setting $v = v_h = w_h$. If the elliptic bilinear form a is symmetric, it represents a scalar product on H, and (2.7) implies that u_h is the best approximation to u with respect to the norm

$$\|u\|_a = \sqrt{a(u,u)}$$

Figure 2.4 illustrates the elementary geometric argument.

Since $c_e\|u\|^2 \leq a(u,u) \leq c_b\|u\|^2$. the error of the best approximation in the standard norm of H is at most by a constant factor larger. This important a priori

bound for Ritz-Galerkin approximations is also valid for non symmetric bilinear forms.

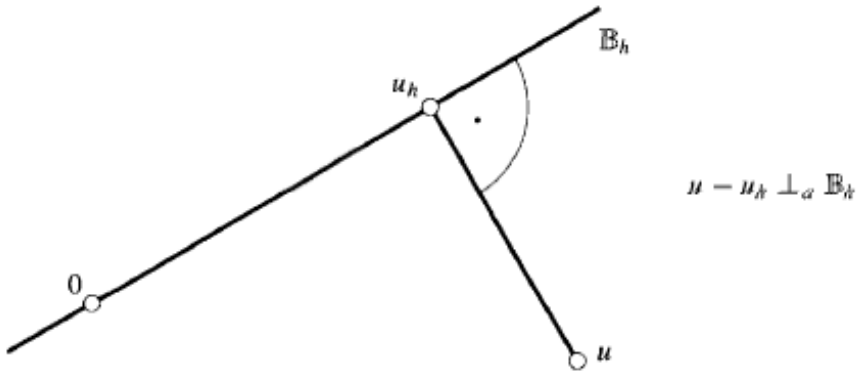

Figure 2.4. *Best approximation* $u_h \in \mathbb{B}_h$ *the scalar product norm* $\|\cdot\|_a$.

Definition 2.7 (Céa's Inequality)
The error of the Ritz-Galerkin approximation $u_h \approx u,$ for an elliptic bilinear form a satisfies

$$\|u - u_h\| \leq c_b/c_e \inf_{u_h \in \mathbb{B}_h} \|u - v_h\|$$

where c_b and c_e are the constants in definition 2.5.

The proof follows from the identity

$$a(u - u_h, u - u_h) = a(u - u_h, u - v_h) \qquad v_h \in \mathbb{B}_h$$

which is a consequence of the orthogonality relation (2.8) with $w_h = u_h - v_h$ By the ellipticity condition 2.6, the left-hand side is $\geq c_e\|u - u_h\|^2$, and the right-hand side is $\leq c_b\|u - u_h\|\|v - v_h\|$. Cancelling the common factor $\|u - u_h\|$ on both sides of the resulting inequality yields the desired estimate since $v_h \in \mathbb{B}_h$is arbitrary.

For piecewise linear Ritz-Galerkin approximations (cf. Figure 2.2) of the model problem (2.1), Cea's inequality implies

$$\|u - u_h\|_1 \leq (c_b/c_e)c\ h\|u\|_2$$

where h *is* the mesh width of the triangulation. In this case, $\|\cdot\| = \|\cdot\|_1$ is the norm of the underlying Hilbert space $H = H_0^1(D)$, and we have used without proof that

$$\|u - v_h\|_\ell \leq c\, h^{2-\ell}\|u\|_2 \quad \ell = 0,1$$

for the best piecewise linear approximation v_h to u. It is sufficient that the triangulations conform to the boundary and are quasiuniform, i.e., that the quotient of the longest and shortest edge is uniformly bounded as $h \to 0$. If the boundary of the polygonal domain D is convex, elliptic regularity yields

$$\|u\|_2 \leq c_r\|f\|_0$$

and we obtain an error estimate entirely in terms of the data of the boundary value problem:

$$\|e_h\|_1 \leq c_1 h\|f\|_0$$

With $e_h = u - u_h$ and $c_1 = (c_b/c_e)cc_r$.

The natural norm $\|\cdot\|$. associated with the boundary value problem, usually involves derivatives. To obtain estimates in weaker norms, such as the L_2-norm $\|\cdot\|_0$ for the model problem, the following result is useful.

Definition 2.8 (Aubin-Nitsche Duality Principle)
If H is a subspace of a Hilbert space H_*, the error $e_h = u - u_h$ of the Ritz-Galerkin approximation satisfies

$$\|e_h\|_*^2 \leq c_b r\|e_h\|$$

where u_* is the solution of the dual problem

$$a(v, u_*) = \langle v, e_h\rangle_*, \qquad v \in H$$

and $\langle\cdot,\cdot\rangle_*$, denotes the scalar product on H_*.

As for Cea's inequality, the proof is based on the orthogonality condition (2.7). We have

$$\langle e_h, e_h\rangle_* = a(e_h, u_* - v_h)$$

for any $v_h \in \mathbb{B}_h$, and the result follows front the boundedness of a.

For the model problem (2.1) we can deduce from theorems 2.7 and 2.8 that

$$\|e_h\|_0 \leq c_0 h^2 \|f\|_0 \tag{2.8}$$

for piecewise linear finite elements on quasi-uniform triangulations of a convex polygonal domain. In this case. $H = H_0^1(D), H_* = L_2(D),\ \|\cdot\|_* = \|\cdot\|_0$, and the two factors in the Aubin-Nitschc estimate can be bounded by

$$\|e_h\|_1 \leq c_1 h \|f\|_0, \qquad r \leq ch\|u_*\|_2$$

respectively. Since $a(v, u_*) = \int_D grad\, u_*\, gradv$, the dual problem is the weak form of

$$-\Delta u_* = e_h \text{ in } D \quad u_* = 0 \text{ on } \partial D.$$

Hence, elliptic regularity implies $\|u_*\|_2 \leq c_r \|e_h\|_0$, proving (2.8) with $c_0 = c_b c_1 (c c_r)$.

The error estimates in this section are completely independent of the particular type of finite elements. In this case,

$$\|u - v_h\|_\ell \leq h^{n+1-\ell} \|u\|_{n+1},$$

Where v_h is the best spline approximation to u of degree $\leq n$ and with grid width h. For second-order problems, Céa's inequality implies that for the $H^1 -$ norm $(\ell = 1)$ this optimal approximation order is retained. This is also the case for the $L_2 -$ norm $(\ell = 0)$ by the Aubin-Nitsche duality principle. However, here we must assume that

$$\|u_*\|_2 \leq c_r \|e_h\|_0$$

i.e., that the dual problem has optimal regularity.

Chapter 3
B-Splines

3.1 The Concept of Splines

Polynomials provide good local approximations for smooth functions. However, on large intervals, the accuracy can be low. Moreover, local changes have global influence. Therefore, it is quite natural to use piecewise polynomials, defined on a partition of the parameter interval *D*. If the break points are uniformly spaced, and the polynomial segments join smoothly, this leads to Schoenberg's classical definition.

Definition 3.1 (Spilnes)
A spline of $degree \leq n$ and grid width h is $(n-1)$-times continuously differentiable and agrees with a polynomial of degree n on each grid interval $[i, i+1]h$ of the parameter interval *D*.

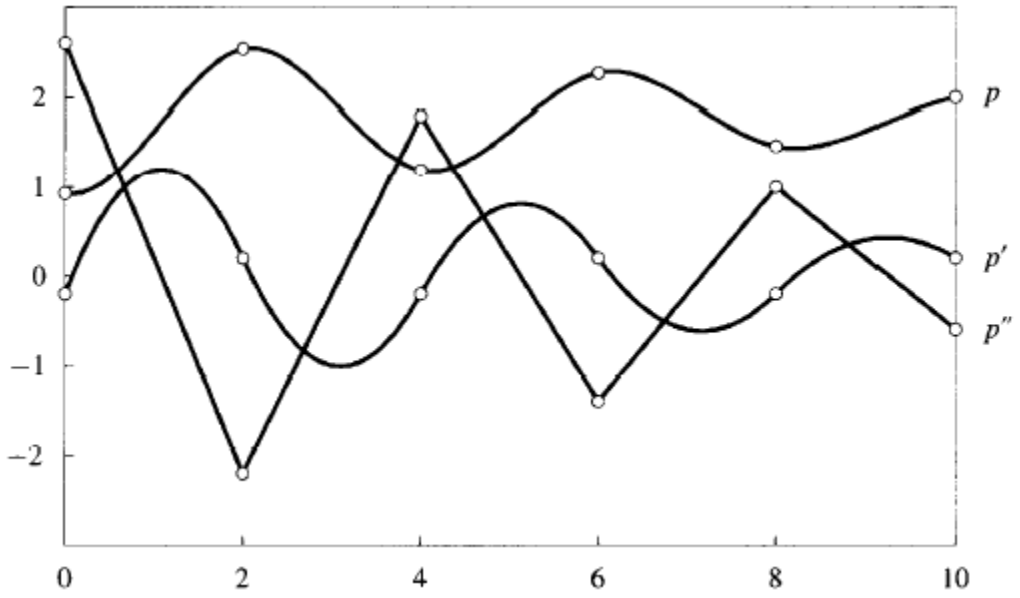

Figure 3.1. *Derivatives of a cubic spline p with grid width* $h = 2$ *and parameter interval* $D = [0,10]$.

Figure 3.1 shows a cubic spline p with five polynomial segments, which, by definition, is twice continuously differentiable. The discontinuities of the third derivative at the break points (marked with circles) are hardly visible. Also the derivative of p, which is a quadratic spline, appears to be smooth. The key to the theory and numerical treatment of splines is the construction of a local basis. The appropriate basis functions, the so-called B-splines, will be defined in the next section. While in hindsight quite simple, the construction is by no means obvious. Therefore, we consider, as a first illustration, the elementary piecewise linear case.

As is apparent in Figure 3.2, a linear spline p is uniquely determined by its values at the break points $x_i = ih$. Hence, it can be represented as a linear combination of hat-functions b_i:

$$p = \sum_i c_i b_i, \quad c_i = p(x_{i+1}) \tag{3.1}$$

The basis functions b_i equal 1 at x_{i+1} and vanish at all other break points. The range of summation depends on the parameter interval D under consideration. As in the example, all hat-functions with some support in D have to be included.

The hat-function basis consists of scaled translates of a single function:

$$b_i(x) = b^1(x/h - i)$$

where the standard hat-function b^1 has support $[0, 2]$ and grid width 1. It is remarkable that

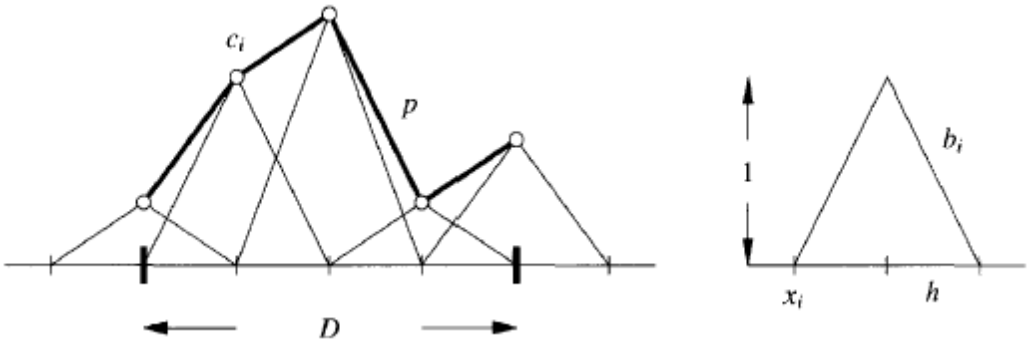

Figure 3.2. *Linear spline p. represented* as *a linear combination of hat-functions* b_i.

this simple structure of the spline space persists in general. For arbitrary degree, splines with uniform break points can be represented in terms of a single B-spline

(cf. definition 3.6).

It should be noted that splines can be defined also for nonuniform partitions and with more general smoothness constraints. The corresponding theory has reached a state of perfection. It provides very flexible approximation methods, in particular when adaptive refinement is necessary. However, most nonuniform techniques are limited to one variable. Therefore, for the construction of finite elements the simpler uniform spline spaces are adequate.

3.2 Definition and Basic Properties

Uniform B-splines can be defined in several ways. We use the following simple averaging process, which makes all basic properties of B-splines immediately apparent.

Definition 3.2 (B-Splines)
The uniform B-spline b^n of degree n is defined by the recursion

$$b^n(x) = \int_{x-1}^{x} b^{n-1}$$

starting from the characteristic function $b^0$of the unit interval $[0, 1)$. Equivalently,

$$\frac{d}{dx} b^n(x) = b^{n-1}(x) - b^{n-1}(x-1)$$

with $b^n(0) = 0$

The first few B-splines are shown in Figure 3.3. One average of the characteristic function yields the piecewise linear hat-function

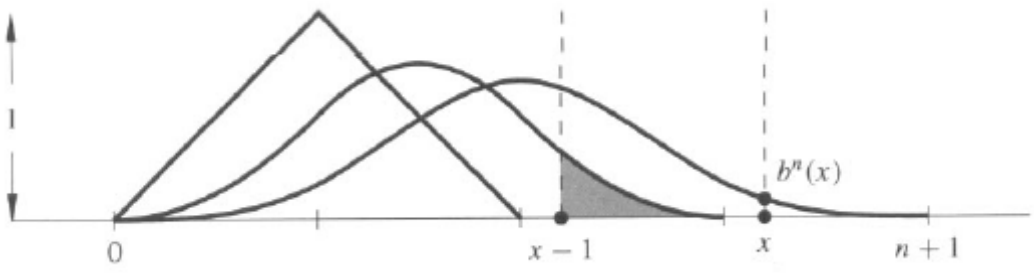

Figure 3.3. *B-splines of degree n* = 1, 2, 3.

$$b^1(x) = \begin{cases} x & \text{for } 0 \le x \le 1, \\ 2 - x & \text{for} 1 \le x \le 2, \\ 0 & \text{other wise} \end{cases}$$

already defined in the previous section. With the next average we obtain the quadratic B-spline b^2. For example, for $x \in [1,2]$,

$$b^2(x) = \int_{x-1}^{x} b^1 = \int_{x-1}^{1} t\, dt + \int_{1}^{x} 2 - t\, dt = -x^2 + 3x - 3/2.$$

The shaded area under the graph of b^2 represents an average $\int_{x-1}^{x} b^2$ yielding a value of the cubic B-spline b^3.

As is illustrated with the examples in the figure, each average increases the length of the support, the smoothness, and the degree by 1. We summarize these basic properties as follows:

- Positivity and local support: b^n is positive on $(0, n+1)$ and vanishes outside this interval.
- Smoothness: b^n is $(n-1)$ −times continuously differentiable with discontinuities of the nth derivative at the break points $0, \dots, n+1$.
- Piecewise polynomial structure: b^n is a polynomial of degree n on each interval $[k, k+1], k = 0, \dots, n$.

Finally, we note two qualitative properties.

Properties 3.3 (Symmetry and Monotonicity)

The B-spline of degree *n* is symmetric that is

$$b^n(x) = b^n(n+1-x)$$

and strictly monotone on $[0, (n+1)/2]$ and $[(n+1)/2, n+1]$.

These properties can be proved by induction on the degree. Assuming that both assertions are valid up to degree $n-1$, it follows from definition 3.2 that

$$b^n(n+1-x) = \int_{n-x}^{n+1-x} b^{n-1}(t)dt = \int_{x-1}^{x} b^{n-1}(n-s)ds = \int_{x-1}^{x} b^{n-1}(s)\, ds,$$

which establishes the symmetry. To show the monotonicity on the left interval, we note that the derivative of b^n.

$$b^{n-1}(x) - b^{n-1}(x-1),$$

is positive for $x \in (0, n/2)$ by induction. This is also true for $n/2 < x < (n+1)/2$ since in this case $b^{n-1}(x) = b^{n-1}(n-x) > b^{n-1}((n-1)/2) > b^{n-1}(x-1)$.

3.3 Recurrence Relation

While definition 3.2 allows us to derive the main properties of B-splines in a straightforward manner, it is not well suited for computations. A simple algorithm for evaluating B-splines is provided by the following recursion, proved by de Boor [2] and Cox [3] more generally for arbitrary break points.

Definition 3.4 (Recurrence Relation)
The B-spline b^n is a weighted combination of B-splines of degree $n-1$:

$$b^n(x) = \frac{x}{n} b^{n-1}(x) + \frac{n+1-x}{n} b^{n-1}(x-1).$$

This recurrence relation is proved by induction, showing the equivalence to the formula for the derivative in definition 3.2. Since both sides of the identity vanish at $x = 0$, it is sufficient to check that the derivatives match. i.e., that

$$b_0^{n-1} - b_1^{n-1} = \frac{1}{n}(b_0^{n-1} - b_1^{n-1}) + \left\{\frac{x}{n}(b_0^{n-2} - b_1^{n-2}) + \frac{n+1-x}{n}(b_1^{n-2} - b_2^{n-2})\right\} \quad (3.2)$$

where we used the abbreviation $b_k^n = b^n(x-k)$. The term in curly braces can be written in the form

$$\frac{n-1}{n}\left(\left[\frac{x}{n-1} b_0^{n-2} + \frac{n-x}{n-1} b_1^{n-2}\right] - \left[\frac{x-1}{n-1} b_1^{n-2} + \frac{n-(x-1)}{n-1} b_2^{n-2}\right]\right),$$

Assuming by induction that the recursion is valid up to degree $n-1$. The terms in brackets $\{...\}$ are equal to $b^{n-1}(x)$ and $b^{n-1}(x-1)$, respectively. Hence,

$$\{\dots\} = \frac{n-1}{n}(b_0^{n-1} - b_1^{n-1}),$$

and both sides of (3.2) agree.

The recurrence relation 3.4 is illustrated in Figure 3.4. We start with hat-functions rather than with the characteristic functions $b^0(\cdot - k)$ to avoid assigning values at break points with discontinuities. In the example, $x \in [1,2]$, so that the rightmost hat-function gives no contribution.

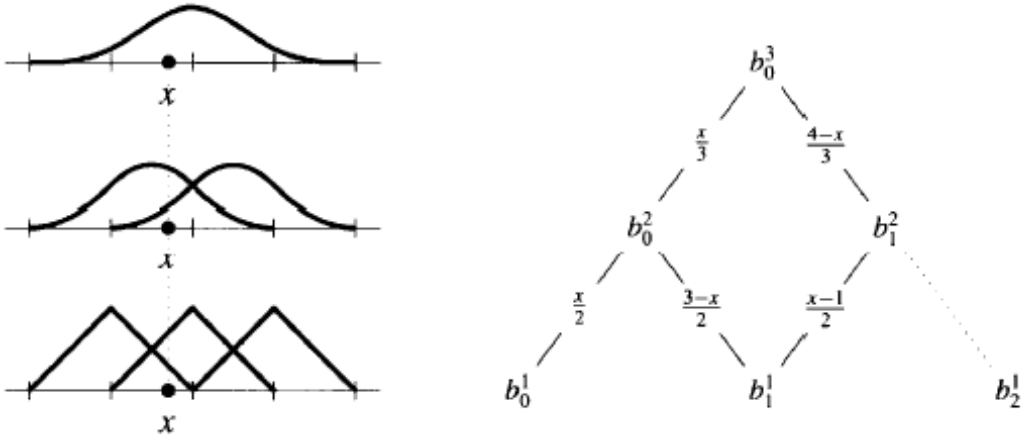

Figure 3.4. *Recurrence relation for a cubic B-spline.*

With the aid of the recurrence relation we can also compute the polynomial segments of the B-splines. This has to be done separately for each grid interval, and it is convenient to use the Taylor expansion with respect to the left break point.

Taylor Coefficients

The $n+1$ polynomial segments

$$a_{k,0}^n + a_{k,1}^n t + \cdots + a_{k,n}^n t^n, \quad t = x - k \in [0,1],$$

of the B-spline b^n can be computed with the recursion

$$a_{k,\ell}^n = \frac{k}{n} a_{k,\ell}^{n-1} + \frac{1}{n} a_{k,\ell-1}^{n-1} + \frac{n+1-k}{n} a_{k-1,\ell}^{n-1} - \frac{1}{n} a_{k-1,\ell-1}^{n-1},$$

starting with $a_{0,0}^0 = 1$ and setting $a_{k,\ell}^n = 0$ if either k or ℓ are $\notin \{0, \dots, n\}$.

For the proof we just have to expand the terms in the recurrence relation 3.4. Restricting $x = k + t$ to the interval $k + [0,1]$ yields

$$\frac{x}{n} b^{n-1}(x) = \left(\frac{k}{n} + \frac{1}{n} t\right)\left(a_{k,0}^{n-1} + a_{k,1}^{n-1} t + \cdots\right),$$

$$\frac{n+1-x}{n} b^{n-1}(x-1) = \left(\frac{n+1-k}{n} - \frac{1}{n} t\right)\left(a_{k-1,0}^{n-1} + a_{k-1,1}^{n-1} t + \cdots\right),$$

Adding the expressions on the right-hand side and collecting the coefficients of t^{ℓ},we obtain the summands in the recursion for $a_{k,\ell}^{n}$.

The Taylor coefficients for the first few B-splines are listed in Table 3.1. For example, the polynomial segments of the quadratic B-splinc ($n = 2$) on the intervals [0,1], [1,2], and [2,3] are

$$\frac{1}{2}x^2, \frac{1}{2} + (x-1) - (x-1)^2, \frac{1}{2} - (x-2) + \frac{1}{2}(x-2)^2.$$

n	1		2			3			
$a_{0,\ell}^{n}$	0	1	0	0	$\frac{1}{2}$	0	0	0	$\frac{1}{6}$
$a_{1,\ell}^{n}$	1	-1	$\frac{1}{2}$	1	-1	$\frac{1}{6}$	$\frac{1}{2}$	$\frac{1}{2}$	$-\frac{1}{2}$
$a_{2,\ell}^{n}$			$\frac{1}{2}$	-1	$\frac{1}{2}$	$\frac{2}{3}$	0	-1	$\frac{1}{2}$
$a_{3,\ell}^{n}$						$\frac{1}{6}$	$-\frac{1}{2}$	$\frac{1}{2}$	$-\frac{1}{6}$

Table 3.1. *Taylor coefficients of the polynomial segments for the B-splines of degree* $n \leq 3$.

When B-splines have to be evaluated repeatedly, using the precomputed Taylor expansions is more efficient than applying the recurrence relation. In particular, this is the case for the assembly of finite element matrices.

3.4 Representation of Polynomials

For the construction of finite element bases in the next chapter, we use scaled translated B-splines. They are defined by transforming the standard uniform B-spline b^n to the grid

$$h\mathbb{Z} : \ldots, -2h - h, 0, h, 2h, \ldots$$

with grid width h. The resulting B-splines $a^n_{k,\ell}$ span the space of smooth splines with uniform knots.

Cardinal Splines
For $h > 0$ and $k \in \mathbb{Z}$,

$$b^n_{k,h}(x) = b^n(x/h - k)$$

are the B-splines on the grid $h\mathbb{Z}$. Their linear combinations $\sum_{k\in\mathbb{Z}} c_k b^n_{k,h}$ are called cardinal splines of degree $\leq n$ with grid width h.

Under the transformation $x \to x/h - k$ the support of b^nchanges to $[k, k + n + 1]h$. This is illustrated in Figure *3.5,* which shows all cubic B-splines with grid width $h = 1/2$ and some support in $[0, 1]$. Moreover, we see that on each grid interval $Q = [\ell, \ell + 1]h$ exactly $n + 1$ B-splines are nonzero.

Identities for b^n generalize easily to the scaled translated B-splines. We just have to incorporate the linear change of variables. For example,

$$\frac{d}{dx} b^n_{k,h}(x) = h^{-1}\left(b^{n-1}_{k,h}(x) - b^{n-1}_{k+1,h}(x)\right) \tag{3.3}$$

follows by scaling the formula for the derivative in definition 3.2.

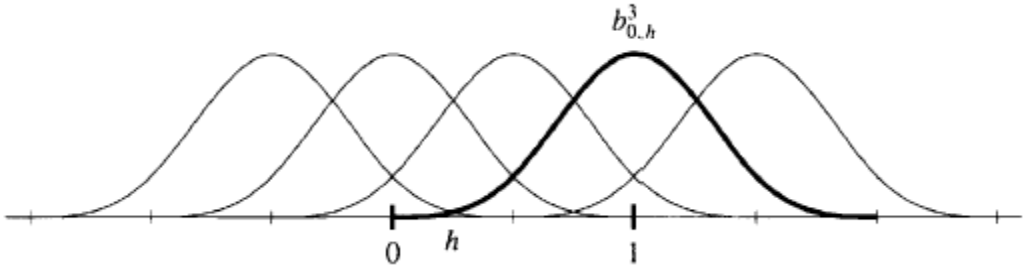

Figure *3.5*. *Scaled translated cubic B-splines.*

We now show that we can represent polynomials as cardinal splines. This property is very important for deriving error estimates.

Marsden's Identity

For $x, t \in \mathbb{R}$.

$$(x-t)^n = \sum_{k\in\mathbb{Z}} \psi_{k,h}^n(t) b_{k,h}^n(x)$$

with $\psi_{k,h}^n(t) = h^n(k+1-t/h) \dots (k+n-t/h)$.

To prove this identity, we make the change of variables

$$x \longrightarrow hx, \quad t \longrightarrow ht,$$

which yields

$$(x-t)^n = \sum_k \psi^n(k-t) b^n(x-k), \qquad \psi^n(s) = (s+1) \dots (s+n)$$

after division by h^n. This formula can be verified by induction. Using the recurrence relation 3.4, we replace $b^n(x-k)$ by

$$\frac{x-k}{n} b^{n-1}(x-k) + \frac{n+1-x+k}{n} b^{n-1}(x-k-1).$$

In the second of the resulting sums over $k \in \mathbb{Z}$ we shift the summation index by 1 $(k \to k-1)$ and obtain the equivalent identity

$$(x-t)^n = \sum_k \left[\frac{x-k}{n}\psi^n(k-t) + \frac{n-x+k}{n}\psi^n(k-1-t)\right] b^{n-1}(x-k) \quad (3.4)$$

By definition of ψ^n the expression in brackets equals

$$\psi^{n-1}(k-t)\left\{\frac{x-k}{n}(k+n-t)+\frac{n-x+k}{n}(k-t)\right\}.$$

A straightforward computation shows that $\{\ldots\} = (x-t)$. Cancelling this factor on both sides of (3.4), we have shown that the identities for degree n and n $-$ 1 are equivalent. Thus, we are left with checking the linear case $n = 1$, where

$$(x-t) = \sum_k (k+1-t)\, b^1(x-k).$$

To this end we observe that the hat-function $b^1(\cdot - k)$ equals 1 at $k+1$ and vanishes at all other integers. Hence, for fixed t, both sides interpolate the same data at the break points $x = \cdots, -1,0,1, \ldots$

Figure 3.6 illustrates Marsden's identity for degree $n = 2$. For the particular choice $t = 0$ and $h = 1$,

$$x^2 = \sum_k (k+1)(k+2)\, b^2(x-k).$$

We have plotted the multiples of the B-splines $b^2(\cdot - k) = b^2_{k,1}$ *for* $k = -6\ldots, 3$ and have also listed the factors $\psi^n_{k,h}(0) = (k+1)(k+2)$.

Marsden's identity yields the representation of any monomial x^ℓ simply by differentiating $(n-\ell)$-times with respect to t, dividing by $(-n) \ldots (-\ell-1)$, and setting $t = 0$. In particular, we have

$$1 = \sum_k b^n_{k,h};$$

i.e., the scaled translated B-splines form a partition of unity.

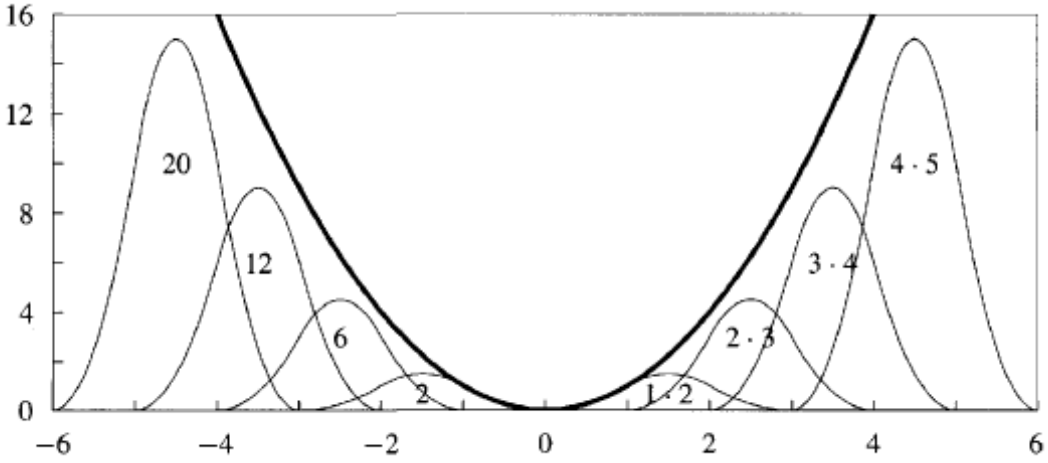

Figure 3.6. Marsden's identity for quadratic B-splines $b^2(x-k)$, $x \in [-6,6]$.

Marsden's identity also implies the linear independence of the B-spline translates.

linear Independence
For any grid interval $Q = [\ell, \ell+1]h$. the B-splines

$$b_{k,h}^n, \qquad k = \ell - n, \dots, \ell$$

which are nonzero on this interval, are linearly independent.

On the interval Q, all polynomials of $degree \leq n$, which span a space of dimension $n+1$, can be represented as linear combinations of the $n+1$ nonzero B-splines.

3.5 Subdivision

Numerical approximations usually involve a sequence of grids in order to judge the accuracy. Mesh refinement is also necessary in a neighborhood of singularities and to resolve small details of solutions. For such purposes the following subdivision formula for B-splines is useful.

Grid Refinement
The B-spline $b_{k,h}^n$ can be expressed as a linear combination of B-splines with grid width $h/2$:

$$b_{k,h}^{n} = 2^{-n} \sum_{\ell=0}^{n+1} \binom{n+1}{\ell} b_{2k+\ell,h/2}^{n} \tag{3.5}$$

This formula is illustrated in Figure 3.7. For a cubic B-spline $b_{k,h}^{3}$ we show the B-splines $b_{2k+\ell,h/2}^{3}$ $\ell = 0, \ldots, 4$, multiplied by their weights $\binom{4}{\ell}/8$. Moreover, we illustrate how the binomial weights can be generated by repeated averaging, a process known as Pascal's triangle.

We prove the subdivision formula (3.5) by induction. The piecewise linear case,

$$b_{k,h}^{1} = \frac{1}{2}(b_{2k,h/2}^{1} + 2b_{2k+1,h/2}^{1} + b_{2k+2,h/2}^{1})$$

is easily checked. We note that both sides interpolate the values

$$0, 1/2, 1, 1/2, 0$$

At $x = kh, kh + h/2, \ldots, kh + 2h$. For the induction step $n - 1 \to n$ *we* differentiate the subdivision formula using (3.3). Since both sides vanish at $x = kh$, this yields the equivalent identity

$$b_k - b_{k+1} = 2^{1-n} \sum_{\ell} \binom{n+1}{\ell} (b'_{2k+\ell} - b'_{2k+\ell+1})$$

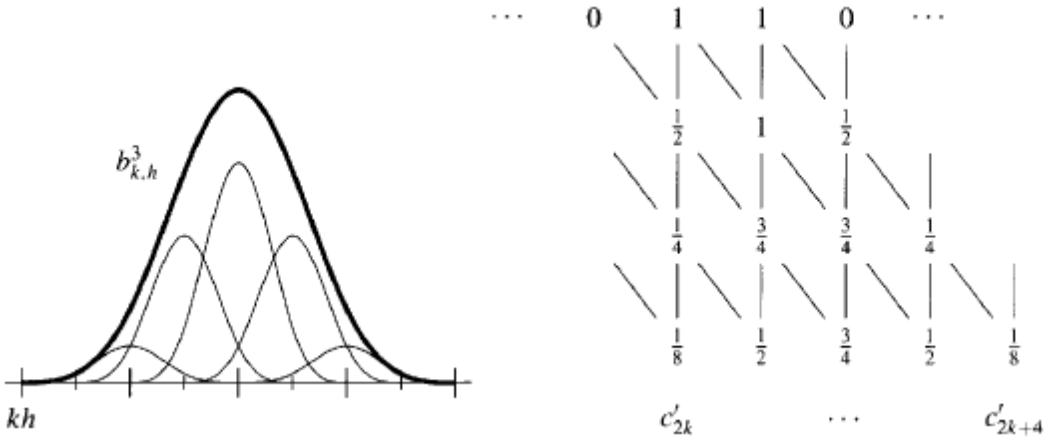

Figure 3.7. *Subdivision of a cubic B-spline.*

where we have set $b_k = b_{k,h}^{n-1}$ and $b'_{\ell,h/2}$ to simplify notation. The factor 2^{-n} has changed since the differentiation formula yields the different factors h^{-1} and $(h/2)^{-1}$ 'for the B-splines on the left- and right-hand side, respectively. Noting that

$$b_{k+1}(x) = b_k(x-k), \quad b'_{2k+\ell}(x-k) = b'_{2k+\ell+2}(x)$$

we rewrite the left-hand side using the induction hypothesis as

$$2^{1-n}\left[\sum_{\ell}\binom{n}{\ell}(b'_{2k+\ell} - b'_{2k+\ell+2})\right].$$

In both expressions in brackets we sum over $\ell \in \mathbb{Z}$, using the convention that $\binom{m}{\ell} = 0$ for < 0 or $\ell > m$.

3.6 Scalar Products

The assembly of finite element matrices involves scalar products of derivatives of B-splincs. As we will show in this section, such integrals can be computed explicitly with the aid of simple identities. We begin with a slightly more general form of the recursion $b^n(x) = \int_{x-1}^{x} b^{n-1}$ for B-splines in definition 3.2.

Theorem 3.5
The convolution of two B-splines is a B-spline of higher degree:

$$b^{m+n+1}(x) = \int_{\mathbb{R}} b^m(x-y)b^n(y)dy$$

For $m = 0$ we recover definition 3.2 since $b^0(x-y)$ equals 1 for $y \in (x-1, x]$ and vanishes outside this interval.

The general case follows by induction on m. Since both sides vanish for $x = 0$, differentiating yields the equivalent equation

$$b^{m+n}(x) - b^{m+n}(x-1) = \int_{\mathbb{R}} \big(b^{m-1}(x-y) - b^{m-1}(x-y-1)\big)b^n(y)dy$$

which is valid by induction hypothesis.

Theorem 5 easily yields a formula for the scalar product

$$\int_{\mathbb{R}} b^n(z/h - k)b^n(z/h - \ell)dz$$

of two B-splines $b_{k,h}^n$ and $b_{\ell,h}^n$. Substituting $y = z/h - \ell$, $dz = hdy$, the argument of the first B-spline becomes $y + \ell - k$. By symmetry we can change this argument to $(n + 1 + k - \ell) - y$. and the convolution formula applies with $x = (\ldots)$. This proves the first part of the following theorem.

Theorem 3.6 Scalar Products

the Scalar Products of he B-splines $b_{k,h}^n$, $b_{\ell,h}^n$ and of their derivatives are

$$s_{k-\ell}^n = h\, b^{2n+1}(n + 1 + k - \ell),$$

$$d_{k-\ell}^n = h^{-1}\left(2s_{k-\ell}^{n-1} - s_{k-\ell-1}^{n-1} - s_{k-\ell+1}^{n-1}\right),$$

respectively.

The formula for the scalar products of the derivatives follows from the differentiation formula (3.3). By the chain rule,

$$h^2 \int_{\mathbb{R}} \frac{d}{dz} b_{k,h}^n(z) \frac{d}{dz} b_{\ell,h}^n(z)dz = \int_{\mathbb{R}} \left(b_{k,h}^{n-1} - b_{k+1,h}^{n-1}\right)\left(b_{\ell,h}^{n-1} - b_{\ell+1,h}^{n-1}\right)$$

and we identify the four scalar products in the formula for $d_{k-\ell}^n$

Table 3.2 shows the scalar products s_v^n and d_v^n up to degree $n = 3$, which are easily generated with the aid of the recurrence relation 3.4. Since, by symmetry, $s_i^n = s_{-i}^n$ and $d_i^n = d_{-i}^n$ only the values with positive index are given.

We can also compute scalar products of higher order derivatives of B-splines. Iterating the differentiation formula (3.3), we obtain

$$\left(\frac{d}{dx}\right)^{\alpha} b_{k,h}^n(x) = h^{-\alpha} \sum_{v=0}^{\alpha} (-1)^v \binom{\alpha}{v} b_{k+v,h}^{n-\alpha}.$$

Hence,

$$\int_{\mathbb{R}} \left(\frac{d}{dx}\right)^{\alpha} b_{k,h}^{n}(x) \left(\frac{d}{dx}\right)^{\beta} b_{\ell,h}^{n}(x)\, dx$$

is a sum of scalar products of B-splines of degrees $n-\alpha$ and $n-\beta$, which, with the aid of theorem 3.5, can he expressed in terms of values of the standard B-spline of degree $2n+1-\alpha-\beta$. We do not discuss this in more detail since such very general formulas are rarely needed in practice.

n	s_0^n s_1^n ...	d_0^n d_1^n ...
1	$\frac{2}{3}$ $\frac{1}{6}$	2 -1
2	$\frac{11}{20}$ $\frac{13}{60}$ $\frac{1}{120}$	1 $-\frac{1}{3}$ $-\frac{1}{6}$
3	$\frac{151}{315}$ $\frac{397}{1680}$ $\frac{1}{42}$ $\frac{1}{5040}$	$\frac{2}{3}$ $-\frac{1}{8}$ $-\frac{1}{5}$ $-\frac{1}{120}$

Table 3.2. *Scalar products of B-splines and their derivatives for* $h=1$.

Chapter 4

Finite element bases

Introduction

In this chapter we construct finite element bases function in regular grids using B-splines. The resulting method provide natural link from geometric modeling numerical simulation they chare all advantages of standard finite element approximation and B-spline representations. In particular, no mesh generation is required, and highly accurate solutions are possible with relatively few parameters.

4.1Multivariate B-splines

There is no unique generalization of univariate B-splines. Several types of multivariate spline spaces have been defined, which differ in the structure f the underlying partition for the polynomial segments. The simplest possibility is to form products of uniform B-splines, as described in the following definition.

Tensor product B-splines

The m-variate B-splines $b_{k,h}^{n}$ with degree n_v in the vth variate, index $k = (k_1, \dots \dots, k_n)$, and grid width h is define as

$$b_{k,h}^{n} = \prod_{v=1}^{m} b_{k,h}^{n_v}(x_v)$$

With the convention that $n_1 = \cdots = n_m$ unless explicitly stated otherwise. For this standard choice, the superscript n is an integer, rather than an integer vector.

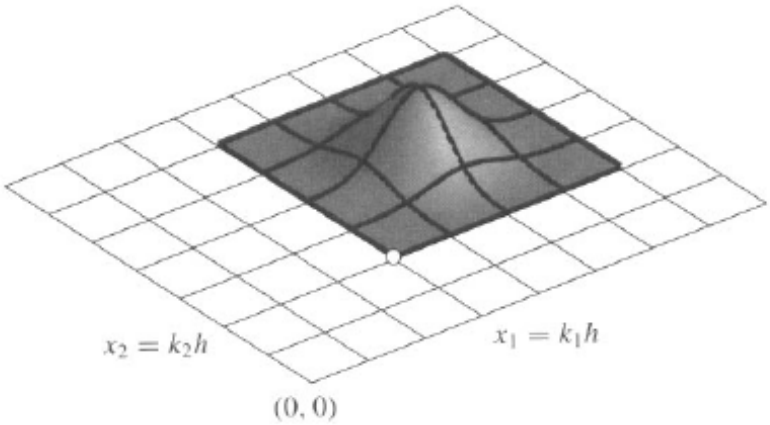

Figure 4.1 *Bicubic B-spline* $(n = 3\ , m = 2)$

Figure 4.1 show a standard Bicubic B-spline $b_{k,h}^3 = b_{(k_1,k_2),h}^{(3,3)}$. We have highlighted the boundary of its support

$$\text{supp} b_{k,h}^3 = [k_1, k_1 + 4]h \times [k_2, k_2 + 4]h$$

and the values along grid lines, which correspond to multiplies of univarite cubic B-splines.

Moreover, we marked the lower left corner kh of the support, which is often used to identify B-splines on the tensor product grid.

From the example in the figure and the definition

$$b_{k,h}^{n_v}(x_v) = b^{n_v}(x_v/h - k_v)$$

Of the scaled translated univariate B-splines, the following properties of the multivariate B-splines with equal coordinate degrees are evident.

- Positivity and local support: $b_{k,h}^n$ is positive on $kh + (0, n + 1)^m h$ and vanishes outside this m-dimentional cube.
- Smoothness: $b_{k,h}^n$ is $(n - 1)$-times continuously differentiable with respect to each variable.
- Piecewise polynomial structure: On each grid cell

$$Q = \ell h + Q_* h, \qquad Q_* = [0,1]^m, \quad \ell = (\ell_1, \dots, \ell_m) \in \mathbb{Z}^m,$$

$b_{k,h}^{n}$ is a polynomial of degree n in each variable, i.e., the B-splines equals

$$\sum_{\alpha_v \le n} c_\alpha x^\alpha, \qquad c_{(n,\dots,n)} \neq 0$$

With $x^\alpha = x_1^{\alpha_1} \dots x_m^{\alpha_m}$.

The general multivariate B-spline with deferent coordinate degrees has analogous properties. However, since we will only need it for representing partial derivative, we preferred to focus on the standard choice $n_1 = \cdots = n_m$.

Because of the product structure of multivariate B-splines, all univariate identities and algorithms generalize easily. As example, we compute partial derivatives. For bivariate B-spline

$$\frac{\partial}{\partial x_1} b_{k,h}^{(n_1,n_2)} = \left[\frac{\partial}{\partial x_1} b^{n_1}(x_1/h - k_1)\right] b_{k_2,h}^{n_2}(x_2)$$

and the univariate differentiation formula (3.3) yields

$$[\dots] = h^{-1}\left(b_{k_1-1,h}^{n_1-1} - b_{k_1+1,h}^{n_1-1}\right).$$

Hence, the partial derivative is a difference of two B-splinces with degree $(n_1 - 1, n_2)$ divided by h. With the familiar multi-index notation

$$\partial^\alpha = \prod_v \partial_v^{\alpha_v},$$

The differentiation formula can be expressed in slightly more compact form as follows.

Theorem 4.1 Partial derivatives

First-order partial derivatives of multivariate B-splines $b_{k,h}^{(n_1,\dots,n_2)}$ are differences of lower degree B-splines, i.e.,

$$\partial^\alpha b_{k,h}^{n} = h^{-1}\left(b_{k,h}^{n-\alpha} - b_{k+\alpha,h}^{n-\alpha}\right)$$

For the unit vectors $\alpha = (1,0,\dots), (0,1,\dots), \dots$.

We can easily compute higher order partial derivatives by iterating the differentiation formula. As an example, we apply the Laplace operator $\Delta = \sum_v \partial_v^2$ to multivariate B-spline. Differentiating the identity in theorem 4.1 yields

$$\partial^\alpha \partial^\alpha = h^{-2}\left(b_{k,h}^{n-2\alpha} - 2b_{k+\alpha,h}^{n-2\alpha}\right) + b_{k+2\alpha,h}^{n-2\alpha}$$

And $\Delta b_{k,h}^n$ is the sum of these expression over all unit vectors α.

As further application, we compute the integrals

$$\mathrm{g}_{k,l} = \int_{\mathbb{R}^m} grad\, b_{k,h}^n grad b_{\ell,h}^n$$

Which appear in the-Galerkin approximation of Poisson's equation, Because of the product form of multivariate B-splines, contriputions from each partial derivative factor, i.e.,

$$\int_{\mathbb{R}^m} \partial_v\, b_{k,h}^n(x)\partial_v b_{\ell,h}^n(x)dx$$
$$= \left(\int_{\mathbb{R}} \partial_v\, b_{k_v,h}^n(x_v)\partial_v b_{\ell_v,h}^n(x_v)dx_v\right)\prod_{\mu\neq v}\int_{\mathbb{R}} \partial_v\, b_{k_\mu,h}^n(x_\mu)\partial_v b_{\ell_\mu,h}^n(x_\mu)dx_\mu.$$

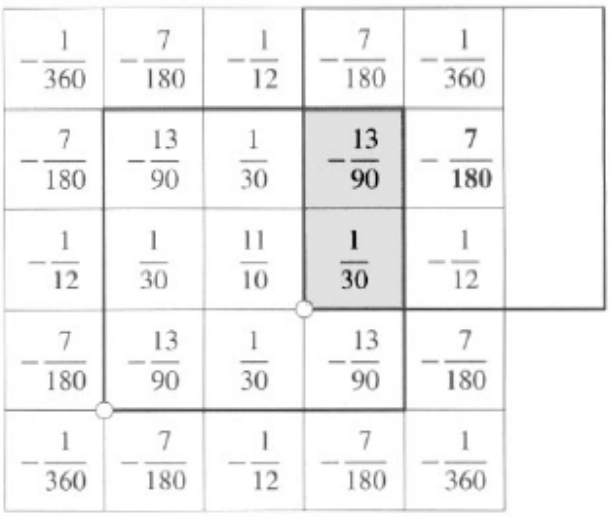

Figure 4.2. Ritz-Galerkin $g_{0,\ell}|\ell_v| \leq 2$, for bi quadratic B-spline.

Hence,

$$g_{k,\ell} = \sum_{v=1}^{m} d^n_{k_v-\ell_v} \prod_{\mu \neq v} s^n_{k_\mu-\ell_\mu}$$

Where $s^n_\cdot$ And $d^n_\cdot$ Are the scalar products define in theorem 3.6 of the previous section.

Figure 4.2 shows the integrals for bi quadratic B-splines. Since $g_{k,\ell}$ depends only on the difference $k-\ell$, we have chosen $k=0$ and associated each value with the center of the support of $b^2_{\ell,h}$. The support of $b^2_{0,h}$ and $b^2_{(2,1),h}$ are highlighted as well as their intersection, which is the region where the scalar product of the gradients is non zero. For this pair of B-splines,

$$g_{k,l} = d^2_{-2}s^2_{-1} + d^2_{-1}s^2_{-2} = -\frac{1}{6}\frac{13}{60} - \frac{1}{3}\frac{1}{120} = -\frac{7}{180},$$

using the values in table 3.2.

4.2 Splines on bounded domains

As first step toward the construction of spline-based finite element subspace, we recall the standard definition of splines as linear combinations of B-splines.

Definition 4.2 (splines)

The splines-$\mathbb{B}_{\mathrm{h}}^{\mathrm{n}}(\mathrm{D})$ on abounded domain $D \subset \mathbb{R}^m$ consist of all linear combinations

$$\sum_{k \in K} c_k b_{k,h}^n$$

Of relevant B-splines; i.e., the set K of relevant indices contains all K with $b_{k,h}^n(x) \neq 0$ for some $x \in D$.

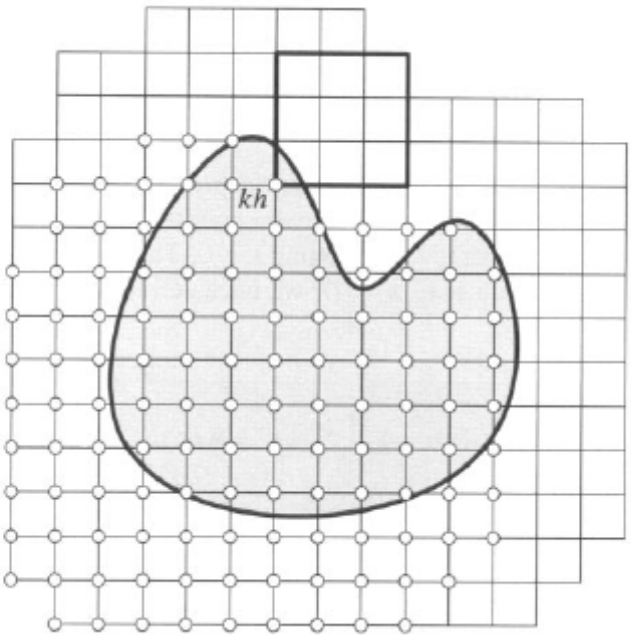

Figure 4.3. *Relevant biquadratic B-splines b_k, $k \in K$, spanning $\mathbb{B}$.*

To simplify notation, For example, we write $\mathbb{B} = \mathbb{B}_h^n(D)$ and $b_k = b_{k,h}^n$.

Definition 4.3 of the spline space $\mathbb{B}$ is illustrated in figure 4.3 for quadratic splines on two-dimensional domain D. the relevant B-splines

b_k, $k \in K$, are marked with circiles at the lower left corner of their support $kh + [0,3]^2 h$ in contrast to univariate splines,$\mathbb{B}$ may contain B- splines with very small support in D; one example is highlighted in the figure. Moreover, depending on the shape of the domain, the set of relevant indices K can be rather irregular. To simplify computations, it is therefore convenient to work with a rectangular array of indices containing K . For analytical arguments we may even sum over $k \in \mathbb{Z}^m$;i.e., we interpret $p \in \mathbb{B}$ as the restriction of an m-variate cardinal spline to D,

$$p(x) = \sum_{\ell \in \mathbb{Z}^m} c_\ell b_\ell(x), \qquad x \in D.$$

This is particularly useful for manipulating sums. Restricting the argument x of the B- splines is simpler than spacefying the minimal summation range.

To obtain accurate approximations, it is crucial that $\mathbb{B}$ contains polynomials. The proof is not difficult and based on Marsden's identity 3.7 restate this univariate formula in the less precise form

$$(x - t)^n = \sum_{k \in \mathbb{Z}} q_h(k, t) b^n(x/h - k),$$

Where q_h is a polynomial of total n in t and k. Forming a product yields the multivariate identity

$$\prod_{v=1}^{m} (x_v - t_v)^n = \sum_{k \in \mathbb{Z}^m} q_h(k, t) b_k(x), \qquad (4.1)$$

Where $q_h(k, t) = \prod_v q_h\,(k_v, t_v)$ is a polynomial of degree n in each of the variables k_v and t_v as in the univarite case, we can compute the representation of any monomial x^α by differentiating (4.1) with respect to t_v and setting $t = 0$. This does not increase the degree of q_h hence, by restricting (4.1) to $x \in D$, we have derived the following multivariate version of Marsden's identity.

Weight functions

At first sight, constructing finite element approximations with B-splines seems infeasible since they do not conform to essential boundary conditions. However, this difficulty can be overcome by multiplying with a weight function w. For example, for Dirichlet boundary conditions w is positive and vanishes on ∂D. The simple idea to use such weighted finite elements was already suggested by Kantorowitsch and Krylow and has become particularly successful. Of course, the *natural* concept also applies to splines. We define the weighted spline space

$$w\mathbb{B}_h^n = \text{span}_{k\in K} w b_k$$

where K is the set of relevant indices.

Chapter 5

Boundary value problems

In this chapter we discuss the approximation of typical boundary value problems with the spline spaces introduced in Chapter 4. All examples fall into the general framework described in Section 2.4: the differential equation for the solution has a weak formulation as a variational problem

$$a(u, v) = \lambda(v), \qquad v \epsilon H,$$

where H is a Hilbert space which incorporates the boundary conditions. The Ritz-Galerkin approximation $u_h = \sum_{i \epsilon I} u_i B_i$ is obtained simply by replacing u by u_h, and v by the bases functions B_k. Although conceptually very straightforward, this approach covers a wide range of applications.

5.1 Essential Boundary Conditions

As a typical model problem we consider Poisson's equation with inhomogeneous Dirichlet boundary conditions:

$$-\Delta\varphi = f \quad in\ D, \qquad \varphi = g \quad on\ \partial D \tag{5.1}$$

This basic boundary value problem describes many physical phenomena. Other examples include heat conduction, electrostatic and magnetic potentials, and fluid flow.

To derive a variational formulation, we first eliminate the inhomogeneous boundary conditions by setting

$$\varphi = u + \tilde{g},$$

Where $u \in H_0^1(D)$ and $\tilde{g}$ is an extension *of* g *to* all of D. *Then* we multiply the differential equation by $v \epsilon H_0^1$ and integrate by parts. This yields

$$\int_D \text{grad } u \text{ grad } v = \int_D fv - \text{grad } \tilde{g} \text{ grad } v\,, \qquad v \in H_0^1$$

as the associated variational problem. Applying the Lax—Milgram theorem 2.6, we obtain the following existence result.

Dirichlet problem

The inhomogeneous Dirichlet problem (5.1). corresponding to the bilinear form

$$a(u, v) = \int_D \text{grad } u \text{ grad } v$$

and the linear functional

$$\lambda(v) = \int_D fv - \text{grad } \tilde{g} \text{ grad } v,$$

has a unique solution $\varphi = u + \tilde{g}$ with $u \in H_0^1$ if f and $grad\ \tilde{g}$are square integrable.

In section 2.4 we have already shown the ellipticity of the Poisson bilinear form on H_0^1. The boundedness of λ is clear from the assumptions on f and $\check{g}$. wenote that the smoothness of the data could be weakened. It is merely necessary that f is a derivative of an L_2-function. While this is not very important from a practical point of view, such precise assumptions play a role in deriving sharp regularity results.

For the Ritz-Galerkin approximation

$$a(u_h, B_i) = \lambda(B_i), \qquad i \epsilon I,$$

we can use any of the spaces $w\mathbb{B}_h, w^e\mathbb{B}_h$ and $w\mathbb{B}_h$, described in Chapter 4, with a weight function of order I which vanishes on all of ∂D. The standard choice are web-splines. The simpler weighted splines $w\mathbb{B}_h$ are adequate for small systems, where stability considerations do not play a significant role.

5.2 Natural Boundary Conditions

While essential boundary conditions have to be incorporated into the solution space, natural boundary conditions are automatically satisfied by weak solutions. As an example, we consider the Neumann problem

$$-\Delta u = f \ \ in\ D \quad , \qquad \partial^{\perp} u = g \ \ on\ \partial D \tag{5.2}$$

Where $\partial^{\perp}$ denotes the normal derivative. i.e. $\partial^{\perp} u$ with the outward unit normal to ∂D. Despite the simplicity of the equations there are some subtle points. From the identity

$$\int_D f = -\int_D \Delta u = -\int_{\partial D} \partial^{\perp} u$$

we see that the data must satisfy the compatibility condition

$$\int_D f = -\int_{\partial D} g \tag{5.3}$$

The necessity of this condition will also become apparent from the physical interpretation in the example discussed below (cf. Figure 5.1). Moreover, a solution is only determined up to an additive constant. These facts have to be taken into account in the associated variational problem.

As usual, we derive the weak formulation by multiplying with a test function *v* and integrating by parts.

$$\int_D gradu\ gradv = \int_D fv + \int_{\partial D} \partial^{\perp} u\, v$$

Having not assumed that v vanishes on ∂D. The boundary conditions for u appear naturally on the right-hand side; i.e., we can define

$$\lambda(v) = \int_D fv + \int_{\partial D} gv.$$

Since λ is bounded:

$$|\lambda(v)| = \|f\|_0 \|v\|_0 + \|g\|_{0,\partial D} \|v\|_{0,\partial D} \leq \|v\|_1.$$

Obviously, the bilinear form

$$a(u,v) = \int_D \text{grad}u\ \text{grad}v$$

is also bounded on H^1. A slight difficulty is that a is not bounded from below since it vanishes on constants. This problem is resolved by working with the subspace

$$H^1_\perp = \left\{u \in H^1 : \int_D u = 0\right\}.$$

Using that the projection $p_0 : u \mapsto \int_D u / \int_D 1$ onto constants is zero on $H^1_\perp$, we have

$$\|u\|_0^2 = \|u - p_0 u\|_0^2 \leq |u|_1^2 = a(u,u).$$

by the Bramble-Hilbert estimate and with $|\cdot|_1$ denoting the Sobolev semi-norm (cf. Section 2.3). Hence, the ellipticity of a on $H^1_\perp$ follows, and we can apply the Lax-Milgram theorem 2.6.

Neumann Problem

The Neumann problem (5.2), corresponding to the bilinear form

$$a(u,v) = \int_D gradu\ gradv$$

and the linear functional

$$\lambda(v) = \int_D fv + \int_{\partial D} gv$$

has a unique solution $u \in H^1_\perp$, provided that the compatibility condition (5.3) is satisfied and f and g are square integrable.

We note that the compatibility condition was not needed to establish the hypothesis of the Lax-Milgram theorem. It is necessary in order to conclude that a sufficiently regular solution of the variational problem solves the boundary value problem (5.2). If (5.3) is satisfied, λ vanishes on constants, so that

$$a(u,v) = \lambda(v) \qquad 3v \in H^1 = H^1_\perp \oplus \{\text{const}\}.$$

Choosing $v \in H_0^1$ proves that $-\Delta u = f$. since in this case the variational equations are identical to those for Poisson's problem. Hence,

$$0 = a(u, v) - \lambda(v) = \int_{\partial D} \partial^{\perp} u v - \int_{\partial D} g v$$

which implies $\partial^{\perp} u = g$ since all test functions $v \in H^1$ are admissible.

The Ritz-Galerkin approximation can be computed with any of the spaces $\mathbb{B}_h$, ${}^{e}\mathbb{B}_h$ (web-splines with $w = 1$), and $\mathbb{B}_h(\mathbb{D})$; a weight function is not necessary. We can ignore that these spaces are not contained in $H_{\perp}^1$, i.e., that the constraint $\int_D u_h = 0$ is not satisfied. Considering, e.g., web-splines (with $w = 1$), we solve the semidefinite system

$$a(u_h, B_k) - \lambda(B_k), \qquad k \in I$$

for $u_h = \sum_{i \in I} u_i B_i$.The compatibility condition guarantees that λ vanishes on constants, so that a solution exists. Subtracting a constant from u_h does not affect the bilinear form, which involves only gradients. Hence, we can select a solution with the proper normalization.

As an application we consider the flow of an incompressible fluid in a channel, as is illustrated in Figure 5.1. If the velocity field V has a potential, i.e., if $V = -gradu$,
then conservation of mass implies

$$div\ V = -\Delta u = 0 \quad (= f).$$

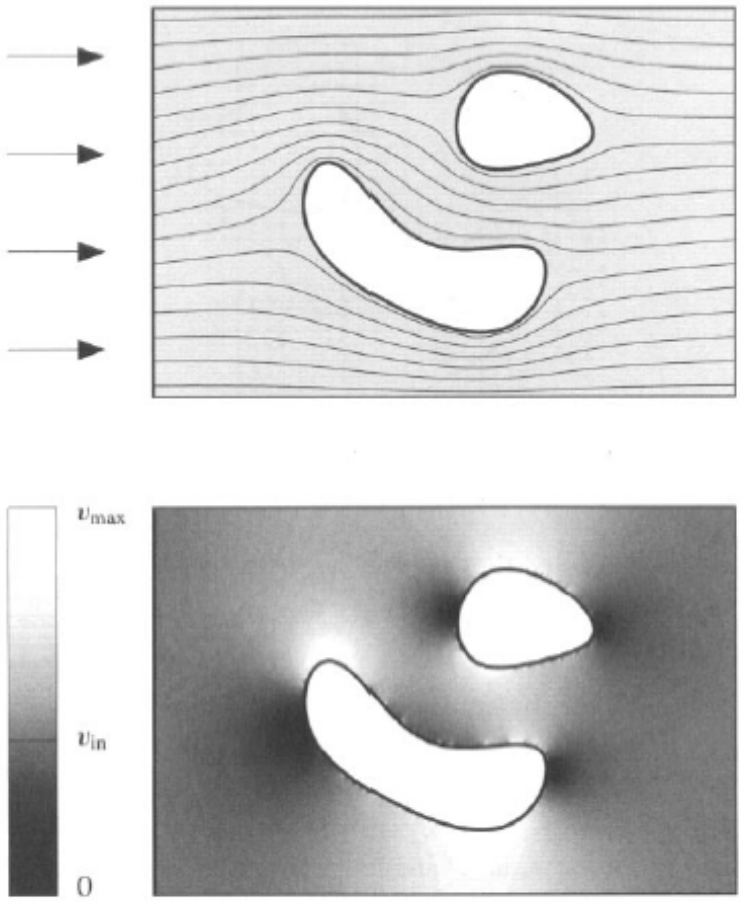

Figure 5.1. *Streamlines (top) and* velocity $\|V\|$ (bottom) of incompressible flow through *a channel with two islands.*

Moreover, the flow rate at the boundary is

$$V\xi = -\partial^{\perp}u \qquad (= -g).$$

In the example of the figure, g equals $v_{in} > O(-v_{in})$ at the left (right) vertical boundaries and is zero at the horizontal and inner boundaries. Here, the compatibility condition $\int_{\partial D} g = 0$ assures that the total mass of the fluid is conserved (inflow = outflow).

The numerical computation of the streamlines is very sensitive. Since the Ritz- Galerkin approximation does not satisfy the natural boundary condition exactly, some of the numerically generated streamlines might intersect the

boundary. Of course, as the grid width becomes small, the percentage of such cases diminishes.

5.3 Linear Elasticity

Models in structure analysis have been the starting point for developing finite element methods. In this application standard finite elements have a natural physical interpretation as small building blocks of elastic materials. Simulations in elasticity still represent today a very important branch of finite element analysis.

The basic physical model is illustrated in Figure 5.1. An elastic solid, occupying a volume $\overline{D}$, is fixed at a portion Γ of its boundary and subject to a volume force on D and a boundary force on $\partial D/\Gamma$ with densities (f_1, f_2, f_3) and (g_1, g_1, g_1), respectively. These forces result in a small deformation of the solid, described by a displacement $u(x) \epsilon \mathbb{R}^3$ of the material points $x \epsilon D$. Typically u is very small, and large distortions indicate excessive forces.

The deformation is determined by minimizing the total energy

$$Q(u) = \frac{1}{2}\int_D \sigma(u) : \varepsilon(u) - \int_D fu - \int_{\partial D/\Gamma} gu \qquad (5.4)$$

over all admissible displacements

$$u = (u_1, u_2, u_3) \in (H_\Gamma^1(D))^3.$$

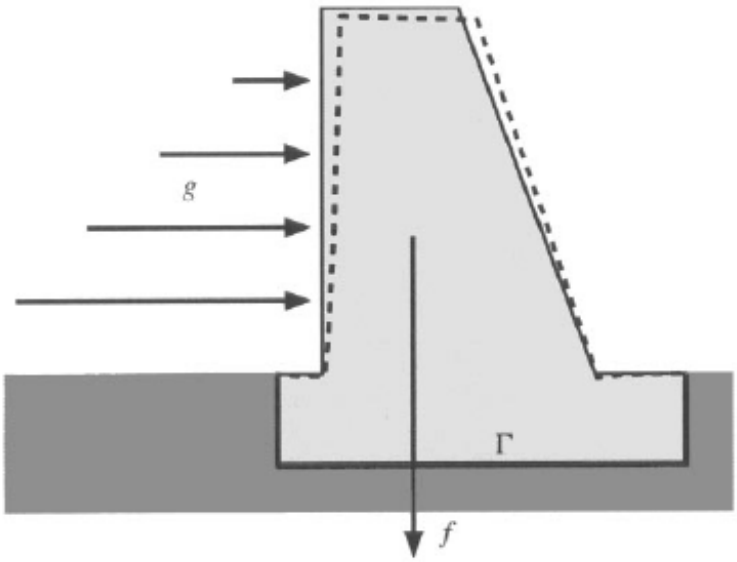

Figure 5.2. *Elastic deformation (magnified) of a dam under lateral pressure and gravitational force.*

with H_Γ^1' the subspace of functions in H^1 which vanish on Γ. Here, σ is the stress and ε the strain tensor, and we used the notation

$$\sigma : \varepsilon = \sum_{k,\ell=1}^{3} \sigma_{k,\ell}\epsilon_{k,\ell}$$

We derivation of the energy functional and merely give the definition of the two symmetric tensors involved:

$$\varepsilon_{k,\ell}(u) = \frac{1}{2}(\partial_k u_\ell + \partial_\ell u_k) \tag{5.5}$$

$$\sigma_{k,\ell}(u) = \lambda \,\text{trace}\, \epsilon(u)\delta_{k,\ell} + 2\mu\epsilon_{k,\ell}(u) \tag{5.6}$$

where trace $\epsilon = \epsilon_{1,1} + \epsilon_{2,2} + \epsilon_{3,3}$. The constants λ and μ are the Lame coefficients, which describe the elastic properties of the material. The second identity, which relates the stress and strain tensor, is known as Hooke's law, valid for an isotropic, homogeneous material.

Writing the first part of the energy functional (5.4) in the form

$\int_D \sigma(u):\varepsilon(u) = \int_D \lambda\,(\text{trace}\,\varepsilon(u))^2 + 2\mu\varepsilon(u):\varepsilon(u)\,, \quad \text{trace}\,\epsilon(u) = \text{div}\,u,$
we see that it corresponds to a symmetric bilinear form $a(u.v)$. Since the integrand involves only first-order derivatives, it is straightforward to establish the boundedness of a in the space $(H_\Gamma^1)^3$, which is equipped with the product norm

$$\|u\|_1 = \left(\sum_{v=1}^{3} \|u_v\|_1^2\right)^{1/2}$$

The derivation of the lower bound, necessary for ellipticity, is much harder. It involves Korn's inequality

$$\|u\|_1 \leq const\ (D)\left(\int_D \varepsilon(u):\varepsilon(u) + uu\right)^{1/2}$$

Moreover, using that u vanishes on Γ. We can eliminate the term $\int uu$ on the right-hand side with the aid of the Poincare-Friedrichs inequality ([4] A.12), Having established the hypothesis of the Lax-Milgram theorem 2.6. We obtain the following familiar result.

Elasticity Problem

The variational problem corresponding to the bilinear form

$$a(u,v) = \int_D \sigma(u):\varepsilon(v)$$

and the linear functional

$$\lambda(v) = \int_D fv + \int_{\partial D\backslash\Gamma} gv$$

with $f \in L_2(D)^3$ and $g \in L_2(\partial D\backslash\Gamma)^3$ has a unique solution $(u_1, u_2, u_3) \in (H_\Gamma^1)^3$

Integrating the variational equations

$$a(u,v) = \lambda(v) \qquad\qquad v\epsilon H_\Gamma^1,$$

by parts (recalling the definition $\varepsilon_{k,\ell}(u) = \frac{1}{2}(\partial_k u_\ell + \partial_\ell u_k)$), it follows that

$$0 = \int_D fv + \frac{1}{2}\sum_{k,\ell}\left[\partial_k \sigma_{k,\ell}(u) v_\ell + \partial_\ell \sigma_{k,\ell} v_k\right] + \int_{\partial D \setminus \Gamma} gv - \frac{1}{2}\sum_{k,\ell}\left[\xi_k \sigma_{k,\ell}(u) v_\ell + \xi_\ell \sigma_{k,\ell} v_k\right],$$

for a sufficiently smooth solution u (ξ denotes the outward normal). Because of the symmetry of σ, the sums of the expressions in brackets are equal in both integrals. For example. the first integral simplifies to

$$\int_D \sum_k \left(f_k + \sum_\ell \partial_\ell \partial_\ell \sigma_{k,\ell} \right) v_k = \int_D (f + div\, \sigma(u)) v.$$

Moreover, arguing, both integrals must vanish separately. Hence, we can read off the boundary value problem associated with the quadratic form (5.4),

$$-div a(u) = f, \quad u = 0 \ \ on\ \Gamma, \quad \sigma(u)\xi = g\ on\ \partial D \setminus \Gamma \tag{5.7}$$

which is referred to as the Lamé-Navier system.

We have assumed that the elastic solid is fixed at a surface $\Gamma \subset \partial D$. However. this need not be the case. The entire boundary could be subject to forces and deformed.

Assembling the Ritz-Galerkin system is slightly more complicated than for scalar problems. Therefore, we discuss it in more detail. Using web-splines as the basis for the finite element subspace, each component u_v, of the vector u is approximated separately by a linear combination

$$(u_h)_v = \sum_{i \in I} u_{i,v} B_i,$$

Where $B_{i|\Gamma} = 0$. Equivalently, we can write

$$u_h = \sum_{i \in I} u_{i,v} B_i,$$

where

$$B_{i,1} = (B_i, 0, 0), \ \ B_{i,2} = (0, B_i, 0), \qquad B_{i,3} = (0, 0, B_i).$$

Hence, the Ritz-Galerkin system $GU = F$ has block structure. The block (k, i) of G is the (3×3)-matrix with entries

$$\int_D \sigma(B_{i,v}) : \varepsilon(B_{i,\ell}), \qquad 1 \le \ell, \qquad v \le 3,$$

and the kth block of the vector F is the 3-vector with components

$$\int_D f B_{k,\ell} + \int_{\partial D \setminus \Gamma} g B_{k,\ell} = \int_D f_\ell B_k + \int_{\partial D \setminus \Gamma} g_\ell B_k, \quad 1 \le \ell \ge 3$$

Since the basis functions $B_{i,v}$ are nonzero in only one component, the tensors σ and ε simplify slightly. For example,

$$\varepsilon(B_{k,1}) = \begin{pmatrix} \partial_1 B_k & \frac{1}{2}\partial_2 B_k & \frac{1}{2}\partial_3 B_k \\ \frac{1}{2}\partial_2 B_k & 0 & 0 \\ \frac{1}{2}\partial_3 B_k & 0 & 0 \end{pmatrix}$$

$$\sigma(B_{i,1}) = \lambda \partial_1 B_i \begin{pmatrix} 1 & 0 & 0 \\ 0 & 1 & 0 \\ 0 & 0 & 1 \end{pmatrix} + 2\mu\varepsilon(B_{i,1}),$$

according to the definitions (5.5) and (5. 6).

$r_\Gamma 2^{-\mu}$, $\mu = 0, \dots, 3$. This system is need to be solved using a Computer program which is not part to in this thesis.

References

[1] P. Bézier (1972), Numerical control-Mathematics and Applications, John Wiley and Sons, New York.

[2] C. de Boor (1972), On Calculating with B-spliens, J. Appro, theory 6: 50 – 62.

[3] M.G. Cox (1972), The Numerical evaluation of B-splines, J. Inst. Math, Appl.

10:134 – 149.

[4] K. Höllig (2003), Finite Element Methods with B-splines, Siam, USA.

[5] J. M. Lane and R. F. Riesenfeld (1980), A theoretical development for the computer generation and display of piesewise polynomial surfaces IEEE Trans. Pattern Anal. Mach. Intelling 2 :35 – 45.

[6] V. L. Rvachev and T.I Skeiko (1995), R-function is boundary value problems in Mechanics, Appl. Mech. Rev. 48: 151 – 188.